THE JOURNAL OF PHYSICAL CHEMISTRY Letters

pubs.acs.org/JPCL Letter

Pressure Effects on Water Dynamics by Time-Resolved Optical Kerr Effect

Andrea Taschin,* Paolo Bartolini, Samuele Fanetti, Andrea Lapini, Margherita Citroni, Roberto Righini, Roberto Bini, and Renato Torre

Cite This: J. Phys. Chem. Lett. 2020, 11, 3063−3068 Read Online

ACCESS | Metrics & More | Article Recommendations | Supporting Information

ABSTRACT: Despite water being the most common and most widely studied substance in the world, it still presents unknown aspects. In particular, water shows several thermodynamic and dynamical anomalies in the liquid and supercooled metastable phases, and the natures of these phases are still hotly debated. Here, we report measurements of water using the optical Kerr effect as a function of pressure along two isotherms, at 273 K from 0.1 to 750 MPa and at 297 K from 0.1 to 1350 MPa, reaching the supercooled metastable phase. The structural relaxation and the low frequency vibrational dynamics of water show a peculiar pressure dependence similar to that of other dynamical properties. The data analysis suggests the presence in the water phase diagram of a crossover area that divides two regions characterized by different dynamic regimes, which appear to be related to two liquid forms, one dominated by the high density water and the other by the low density water.

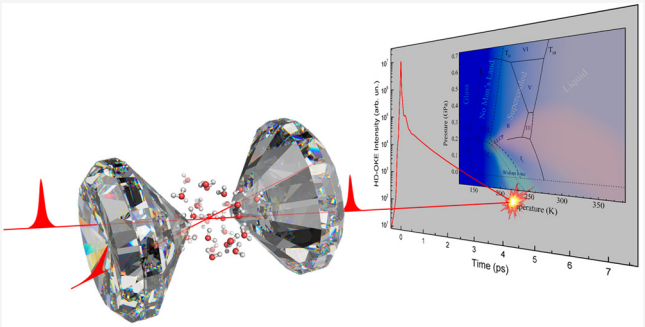

Water shows a series of unexpected physical properties both in liquid and metastable phases;[1] despite the different physical models and thermodynamic interpretations proposed,[2] the origin of these anomalies is still unclear and the subject of an intense debate.[3−7] It is widely accepted that water anomalies are connected to the local structural arrangement, characterized by a temperature and pressure dependent degree of order that affects the dynamic properties[7,8] of the liquid. Among the several theoretical models proposed,[2] the second critical point (SCP) hypothesis[9] is the most accredited and debated. This model hypothesizes the existence of a first order phase transition between the low-density (LDW) and high-density (HDW) water forms; the low-density phase is characterized by tetrahedral intermolecular coordination, while the high-density one shows more closely packed structures with a distorted hydrogen bond network. The phase transition would exist only in the deep supercooled phase and would terminate in a liquid−liquid critical point (LLPC). The predictions of the SCP model are supported by a series of computational results and are compatible with many experimental results;[2,10,11] nevertheless, the crystallization process limits the experimental investigations in a phase diagram region where the observed anomalous properties cannot be exclusively attributed to the LLCP existence.

In this scenario, continuous efforts aim to realize new experimental investigations to unravel the water mystery, leading liquid water beyond the metastable phase limit[12,13] and/or measuring new unexplored physical observables.[14,15] The high pressure states of liquid water certainly represent an unexplored region of the phase diagram that can give new valuable information. The pressure dependence of different dynamical properties of water has been the subject of several investigations.[16−25] All of these experimental studies evidenced the pressure variation of several dynamical parameters along the isotherms that was attributed to changes of the local structural arrangement. The nature of these anomalies remains not fully explained, but it is accepted that they are related to the pressure induced collapse of the second molecular solvation shell into the first one, correlated with the conversion from LDW to HDW water form; nevertheless, the connection between these phenomena and the LLCP hypothesis has not yet been clarified.

Recently, the thermodynamic and dynamical anomalies of water were successfully explained by the two-state model,[3,10,25−31] which describes water as an athermal nonideal solution of two states, or structures, that quickly interconvert. The mixing ratio of the two species is a function of temperature and pressure. At low temperatures, the system undergoes a phase separation in two different liquids, which terminates at a liquid−liquid critical point. The success of the

Received: February 3, 2020
Accepted: March 26, 2020
Published: March 26, 2020

two-state model reinforces the description of pure water as a bimodal distribution of local structures against the continuous model, in which all local structures should exist with equal probability. In the two-state picture, the coexistence of the LDW and HDW forms should not be seen as resulting from static inhomogeneity of the liquid but rather due to the equilibrium between rapidly (on the molecular time scale) interconverting local structures. A direct measurement of structural dynamics can provide valuable information on water modeling, in particular on the diatribe between bimodal and continuous structuring.

Here, we report on the investigation of water dynamics as a function of pressure at 273 K and at 297 K. We used a nonlinear time-resolved spectroscopic technique, the heterodyne detected optical Kerr effect (HD-OKE) experiment.[32] In most simple molecular liquids, the relaxation of the OKE signal is interpreted in terms of single molecule orientational diffusion; on the contrary, the anisotropy of the molecular polarizability of water is so low that the optically induced polarization is dominated by intermolecular contributions. Thus, the long time decay of the measured signal of liquid water is associated with the rearrangement of hydrogen-bonded extensive structures, i.e. with the first step of the structural relaxation. In parallel, the short time part of the signal accounts for the intermolecular vibrational dynamics, which provides additional information on the collective behavior of the liquid. The technique allows measuring the structural relaxation processes and the low frequency vibrational dynamics of water with unprecedented data quality.[14,32,33] This is the first time that HD-OKE was used to study compressed water. The only attempt, so far reported in the literature, to measure OKE on a pressurized liquid concerned carbon disulfide,[34] whose nonlinear signal is orders of magnitude stronger than that of water. Moreover, HD-OKE measures the water collective dynamics that remains poorly explored at high pressure due to the intrinsic experimental difficulties; only viscosity[25] and water sound velocity have been investigated so far.[35,36] For the analysis of the experimental results, we adopted the two state model, following the approach proposed by Singh et al.[25] for the interpretation of the pressure dependence of other dynamic observables of water.

In the HD-OKE experiment, a polarized short laser pulse (the pump) induces a transient optical birefringence in the sample, corresponding to the coherence of vibrational and rotational/librational states induced via stimulated Raman coupling.[37] The time evolution of the induced birefringence, due to the relaxation of those coherent states, is monitored by a second delayed laser pulse (the probe). The experiment measures the third order response function, which is directly connected to the time derivative of the correlation function of the first order anisotropic susceptibility. The measured signal contains information on the diffusion/relaxation processes and on the low-frequency vibrational dynamics of the sample. The laser pulses, centered at the wavelength of 800 nm, have a duration of 18 fs (more experimental details can be found in the Supporting Information Section S.1.2, and in ref 32). Recent experimental improvements provide access to a very large time/frequency window, covering the whole intermolecular water dynamics.[32] Nevertheless, the extraction of the water response function from the intrinsically very weak HD-OKE signal is far from being a trivial procedure and relies on the knowledge of the appropriate instrumental function and on the consequent correct deconvolution of the HD-OKE signal (see Section S.1.4 for more details). We performed the high pressure experiments on bidistilled water samples held in a diamond anvil cell (DAC) with a gasket having initial thickness of ∼250 μm and initial diameter of ∼500 μm (see Section S.1.1 of the Supporting Information). Temperature has been controlled by means of a nitrogen continuous-flow cryostat equipped with a thermocouple fixed on the sample cell (accuracy of ±0.1 K). The sample pressure was determined by the ruby fluorescence technique; for this purpose, a small ruby chip was loaded in the cell together with the sample. For the room pressure measurements, we used water provided by Angelini company (see ref 14), sealed in a cylindrical glass vial (see Section S.1.1 of the Supporting Information).

We measured the water dynamics along two isotherms: at T = 297 K the pressure varies from 0.1 MPa to 750 MPa, at T = 273 K from 0.1 to 1350 MPa. The HD-OKE signal, measured at two different pressures and temperatures, is reported in Figure 1. The data show the intermolecular vibrational

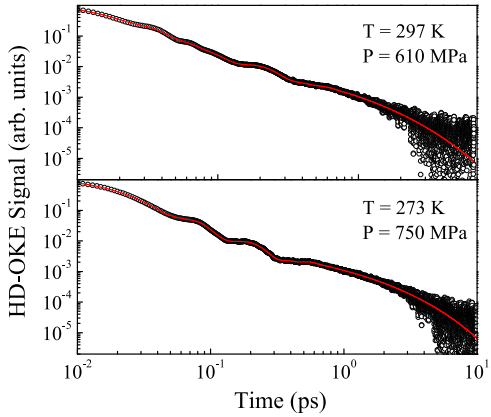

Figure 1. HD-OKE signals measured at two different pressures for the two isotherms. The signal shows, at short times (<1 ps), fast oscillations due to the intermolecular vibrational dynamics and, at longer times, the monotonic decay due to structural relaxation.

dynamics, extending up to about 1 ps, merging into the structural relaxation that lasts longer.[14,33] The structural relaxation changes with the applied pressure; initially, the relaxation gets faster as pressure increases, while it slows in consequence of further pressure increments. The effect of pressure on the oscillating part of the signal is less evident in the time-domain data, but it becomes clear in the data transformed to the frequency domain, as it will be shown in the following.

The deconvolution process of the time domain HD-OKE signal implies the knowledge of the instrumental function and requires some assumption on the form of the water response function. The two tasks are of different complexity, depending on the theoretical model used. Data analysis with complex theoretical models, such as those we used to study supercooled water at ambient pressure in the framework of the mode coupling theory (MCT),[14,32] requires data of very high quality. The method adopted here is definitely less demanding. We assumed (see Section S.1.3 of the Supporting Information) a relatively simple response function based on a phenomenological approach: the slow decay is simulated by the time derivative of a stretched exponential and the vibrational/oscillatory part by the time derivative of two damped harmonic

https://dx.doi.org/10.1021/acs.jpclett.0c00363
J. Phys. Chem. Lett. 2020, 11, 3063−3068

oscillators (see Supporting Information, Section S.1.3). For what concerns the instrumental function, we built a kind of "artificial" function from the rising profile of the electronic peak of the HD-OKE signal (see Supporting Information, Section S.1.4). As shown in Figure 1, the used response function fits very well the measured signal in the entire time window.

The frequency domain response function $\tilde{R}(\omega)$ is obtained as the Fourier transform of the HD-OKE signal $S(t)$. The required deconvolution of the raw data is performed making use of the relation: $\mathrm{Im}[\tilde{R}(\omega)] \propto \mathrm{Im}\{FT[S(t)]/FT[G(t)]\}$,[32,37] where $G(t)$ is the instrumental function. Two examples of the frequency response function $\mathrm{Im}[\tilde{R}(\omega)]$ are reported in Figure 2. These spectra correspond to the low-frequency depolarized

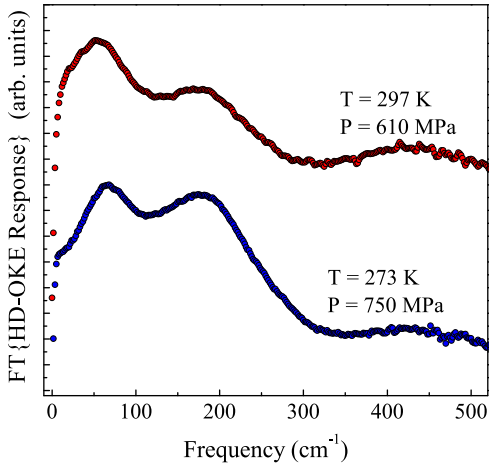

Figure 2. HD-OKE response in the frequency domain, $\mathrm{Im}[\tilde{R}(\omega)]$, obtained as the Fourier transform of the time-dependent data shown in Figure 1, after the contribution of the instrumental function has been removed in the deconvolution process.

Raman signal, corrected for the Bose factor; they consist of two bands due to intermolecular vibrations. The assignment of the corresponding modes is not obvious; according to a series of computational investigations,[38−41] the 60 cm^{-1} broad band is dominated by transverse translational motions, corresponding to "bending" of the hydrogen bonds; the 180 cm^{-1} involves motions with essentially longitudinal character, i.e. H-bond "stretching". The slow decay of the OKE signal measured in the time domain corresponds to the very low frequency shoulder that is hardly visible in the reported spectra.

The slow decay of the signal is fairly well-reproduced by the derivative of the stretched exponential. Due to the difficulty of obtaining a reliable value of the stretching exponent, we decide to fix it to the room pressure value of 0.6.[33] The mean structural relaxation time (see Section S.1.3 of the Supporting Information) extracted from the fit was analyzed as a function of pressure. As already reported in the literature for other dynamical properties, namely self-dynamics, self-diffusion constant, rotational correlation time, and viscosity,[16−23,25,42,43] the structural relation time also shows an anomalous trend with increasing pressure. Specifically, it decreases when pressure is applied, reaches a minimum, and then increases with the density, following the usual trend of "normal" liquids. The pressure value at the minimum changes with the temperature. This anomalous behavior can be further emphasized by plotting the mean structural times as a function of density, as shown in Figure 3. The density values were

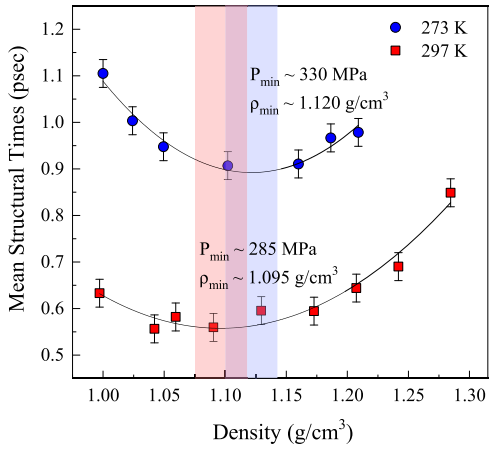

Figure 3. Mean structural relaxation times (see Section S.1.3 of the Supporting Information) at the densities corresponding to the different applied pressures, obtained from the fit of the slower part of the HD-OKE data with a stretched exponential, for the two isotherms. The structural relaxation time shows an anomalous trend with the density: it decreases with application of pressure, reaches a minimum (at a density value that increases with decreasing temperature), and then increases again. Light red and light blue shadowed bands represent the density (pressure) ranges where the minimum can be positioned at the higher and lower temperatures, respectively.

computed from the equation of state of water.[52] For the two studied isotherms (297 and 273 K), a polynomial fit locates the minimum values of the two curves of Figure 3 at the densities of about 1.095 and 1.120 g/cm^3, respectively, corresponding to pressure values of about 285 and 330 MPa.

Similar crossover points can be found in the fitting parameters of the oscillating part of the HD-OKE signal. This part, as stated above, is fairly well-reproduced by two damped harmonic oscillators (DHOs), corresponding to the two low frequency bands shown in the spectra of Figure 2 around 60 and 180 cm^{-1}. The density dependence of the bending and stretching frequencies (frequency Ω_n of the DHO, see Supporting Information, Section S.1.3) for the two isotherms 297 and 273 K is shown in Figure 4 and Figure 5, respectively. For the 297 K isotherm, in both bands we can identify two linear regimes with different slopes. The values of the density at which the slope changes occurs are around ρ = 1.100 g/cm^3 for the stretching band and ρ = 1.090 g/cm^3 for the bending, values that correspond to pressures of about 295 and 260 MPa. At the lower temperature, 273 K, instead, the crossover is clearly visible only in the bending band. The determination of the frequency of the stretching band at the lower temperature is more critical; this is due to the large overlap of this band with those at higher frequency, namely the librational contributions, leading to a poorly reliable estimation of the stretching band parameters. In summary, our results clearly identify, at both temperatures, a dynamic crossover for the structural relaxation time. The same is true for the bending peak, while for the stretching band, the bimodal behavior is observed only at 297 K.

The scaling proprieties of the structural relaxation time in liquids have been often evaluated using the Stokes−Einstein−Debye models; for liquid water, those simple models cannot describe correctly the pressure/temperature dependence of the relaxation times.[45,46] In Section S.2 of the Supporting

https://dx.doi.org/10.1021/acs.jpclett.0c00363
J. Phys. Chem. Lett. 2020, 11, 3063−3068

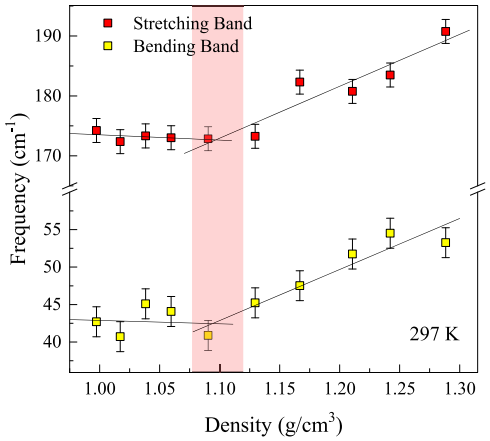

Figure 4. Frequency of bending and stretching peaks at variable densities extracted from the analysis of the HD-OKE signal at 297 K based on two DHOs. Both frequencies show two linear regimes with different slopes; the crossover points are close to that of the structural time in Figure 3. The shadowed band represent the density range where the crossover point can be located based on data errors.

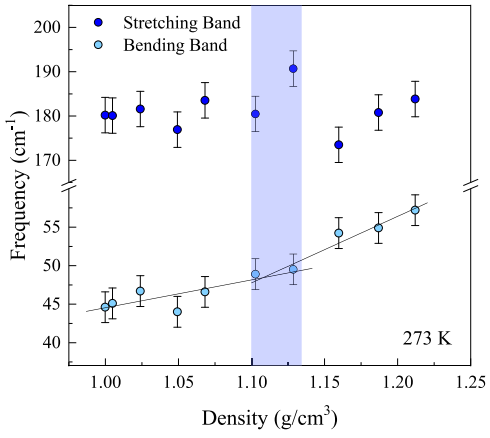

Figure 5. Frequency of bending and stretching peaks at variable densities extracted from the analysis of the HD-OKE signal at 273 K based on two DHOs. The frequency of the bending band shows two linear regimes with different slopes with a crossover point close to that of the structural time in Figure 3. No well-defined trend can be identified for the stretching frequency. The shadowed band represents the density range where the crossover point can be located based on data errors.

Information, we report a short discussion on the application of these models to our data.

It is interesting to verify if the trend with pressure of our relaxation times can be described by the two state model.[3,10,25,29,30] As we mentioned in the introduction, they describe the liquid water as an athermal nonideal mixture of two states/structures characterized by different entropies and densities: the LDW and the HDW states. A key parameter of the model is $f(T, P)$, the fraction LDW/(HDW+LDW). This two-state model was utilized by Singh et al.[25] to describe some dynamic observables of water (viscosity, diffusivity, and rotational time) and their pressure dependence. In this picture, the dynamic observable is governed by an effective activation energy, which is an average of the activation energies of the LDW and HDW state, weighted by the fractions f and $1 - f$, respectively. Following this approach, the relaxation time can be written as

$$\tau(T, P) = \tau_0\left(\frac{273.15}{T}\right)^{0.5} \times \exp\left\{[1 - f(T, P)]\frac{E_{HDW} + \Delta\nu_{HDW}P}{k_B(T - T_0)} + f(T, P)\frac{E_{LDW}}{k_B T}\right\} \quad (1)$$

In eq 1, water dynamics is treated as that of a mixture of a strong liquid, LDW, with a highly tetrahedral hydrogen bond network, and a fragile liquid, HDW, with a more disordered and close packed structure. The LDW structure is only weakly affected by pressure, and its relaxation time follows an Arrhenius law with E_{LDW} activation energy. The relaxation of the HDW liquid follows a Vogel−Tamann−Fulcher law with a critical temperature T_0 and a pressure dependent activation energy $E_{HDW} + \Delta\nu_{HDW}P$, $\Delta\nu_{HDW}$ being the volume difference between the activated and initial states. For the calculation of the $f(T, P)$ fraction, we used the code reported in the Supporting Information of ref 29 (see Section S.3 of the Supporting Information). We kept the parameter T_0 fixed at 148 K, the value obtained in the analysis reported in ref 25. With this constraint, the free fitting parameters were E_{LDW}, E_{HDW}, and $\Delta\nu_{HDW}$. The curves in Figure 6 are the best fit

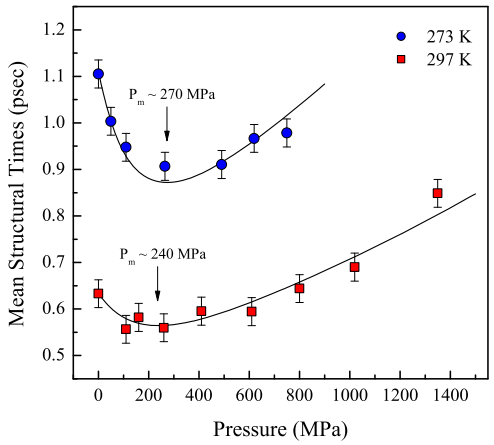

Figure 6. Structural relaxation times (scatter point) as a function of pressure for the two isotherms compared with theoretical values calculated according to the two state model (continuous lines).

prediction of the two state model, obtained with E_{LDW}/k_B = 1800 ± 300 K, E_{HDW}/k_B = 280 ± 50 K, and $\Delta\nu_{HDW}$ 0.75 ± 0.2 × 10^{-30} m^3, values of the same order of magnitude as those reported by Singh et al.[25] in their calculation of different dynamical properties. The curves reproduce fairly well the pressure dependence of the experimental mean structural relaxation times, the minima of the two curves being located at 270 and 240 MPa for 297 and 273 K, respectively. Both of these values are 50 MPa lower than those obtained from the data analysis of Figure 3 and, most importantly, preserve the same ordering. The pressure/temperature dependence of the present structural relaxation data are in good agreement with the two state model, cast into eq 1; therefore, we can affirm that these data push the balance forward to a bimodal interpretation of liquid water structures, persisting even at room temperature and high pressure conditions.

https://dx.doi.org/10.1021/acs.jpclett.0c00363
J. Phys. Chem. Lett. 2020, 11, 3063−3068

It is worth comparing our results with other data present in the literature. In the temperature−pressure phase diagram of water of Figure 7, we report the loci for the extrema of several

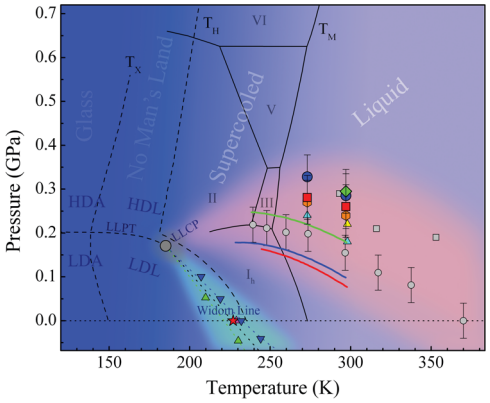

Figure 7. Schematic temperature−pressure phase diagram of water: T_M, melting line; T_H, homogeneous nucleation line; T_X, amorphous ice crystallization line. The HD-OKE investigation in ref 14 individuates the critical point at atmospheric pressure (red star); the HD-OKE measurements along the two isotherms define the dynamic crossover points: thermodynamic points of the minimum of structural relaxation time (blue circles), slope change values of the frequency of the bending band (red squares), the frequency of the stretching band (green diamond), and the minimum of structural relaxation time extracted from the two state model (orange hexagons). Moreover, extrema of the following dynamical properties are shown: slope change of the rotational anisotropy time constant (yellow triangle),[22] slope change of the OD stretching vibrational lifetime (cyan triangles),[22] the slope change of the water stretching band as measured by FTIR (gray circles),[23] sound velocity from Brillouin scattering (gray squares),[36] self-diffusion coefficient (blue line),[25] rotational correlation time (green line),[25] and viscosity (red line).[25] Finally, extrema of isothermal compressibility (blue triangles) and specific heat (green triangles) calculated from the simulations[47] experimental value of the maximum of isothermal compressibility at room pressure (magenta triangle)[11] are shown. The ensemble of data points of different origin identify two regions: the narrow greenish area coincides with the Widom line emanating from the LLCP; the much broader reddish area contains the crossover lines measured for different observables.

dynamical properties found in literature[22,23,25,36] together with our crossover points. All data points are located close to the area where simulations predict the structural transition between the two water forms and the pressure induced collapse of the second shell on the first one. In the same phase diagram, we report the extrema of isothermal compressibility and specific heat calculated from the simulations,[47] and the maximum of the isothermal compressibility measured at room pressure.[11] These data points are in the vicinity of the Widom line,[11,48] which is the continuation of the liquid−liquid phase transition line and emanates from the LLCP in the supercritical region. On the same Widom line, a few studies place the strong-to-fragile dynamics crossover,[49] yet on the same line is the critical temperature T_C of MCT obtained from our OKE data on supercooled water[14] (red star in Figure 7). Within the LLCP scenario, the Widom line and dynamical crossover points possibly identify two critical areas that could be both related to the liquid−liquid critical point. Computer simulation studies on liquids with tetrahedral symmetry[50] found that two Widom lines can arise from the same LLCP, one with positive slope in the $P-T$ thermodynamic plane and another one with negative slope. On the other hand, another molecular-dynamics simulation study on high pressure water[51] attributes the dynamical crossover to the LD-HD conversion, the latter being just the structural precursor of the high density ice(s). Therefore, in this scenario, the line would head toward some high density ice phase transition line and would be unrelated to the hypothetical LLCP.

In summary, our findings concerning both structural relaxation dynamics and vibrational dynamics evidently confirm the presence of a dynamical crossover to be related to the structural change of water at different pressures and temperature conditions. The interpretations of these crossover phenomena for the structural relaxation and viscosity observables are in fair agreement with the two state model, showing these crossovers could be in fact the emanation of LLCP point at high temperature/pressure. In this framework, the bimodal model of water would only be the extension of the LL model at the noncritical thermodynamic conditions, where the HD and LD water phases become local transient fluctuations of the network structure. Nevertheless, other experimental investigations are required to definitively determine the proper model for liquid water. In this respect, the feasibility, demonstrated in the present work, of accurate time-resolved OKE experiments on pressurized water in anvil cells opens an interesting perspective for the experimental study of collective dynamical properties of aqueous samples.

■ ASSOCIATED CONTENT

Supporting Information

The Supporting Information is available free of charge at https://pubs.acs.org/doi/10.1021/acs.jpclett.0c00363.

Detailed description of the sample preparation, the DAC cell, the experimental technique, and the data analysis (PDF)

■ AUTHOR INFORMATION

Corresponding Author

Andrea Taschin − *European Laboratory for Non-Linear Spectroscopy (LENS), Università di Firenze, I-50019 Sesto Fiorentino, Firenze, Italy;* orcid.org/0000-0003-4088-7964; Email: taschin@lens.unifi.it

Authors

Paolo Bartolini − *European Laboratory for Non-Linear Spectroscopy (LENS), Università di Firenze, I-50019 Sesto Fiorentino, Firenze, Italy*

Samuele Fanetti − *European Laboratory for Non-Linear Spectroscopy (LENS), Università di Firenze, I-50019 Sesto Fiorentino, Firenze, Italy; ICCOM-CNR, Istituto di Chimica dei Composti OrganoMetallici, Consiglio Nazionale delle Ricerche, I-50019 Sesto Fiorentino, Firenze, Italy;* orcid.org/0000-0002-5688-6272

Andrea Lapini − *European Laboratory for Non-Linear Spectroscopy (LENS), Università di Firenze, I-50019 Sesto Fiorentino, Firenze, Italy; INRIM, Istituto Nazionale di Ricerca Metrologica, I-10135 Torino, Italy;* orcid.org/0000-0002-2204-7673

Margherita Citroni − *European Laboratory for Non-Linear Spectroscopy (LENS), Università di Firenze, I-50019 Sesto Fiorentino, Firenze, Italy;* orcid.org/0000-0001-8555-1263

Roberto Righini − *European Laboratory for Non-Linear Spectroscopy (LENS) and Dipartimento di Chimica "Ugo*

https://dx.doi.org/10.1021/acs.jpclett.0c00363
J. Phys. Chem. Lett. 2020, 11, 3063−3068

Schiff", Università di Firenze, I-50019 Sesto Fiorentino, Firenze, Italy; orcid.org/0000-0003-0260-0248

Roberto Bini − *European Laboratory for Non-Linear Spectroscopy (LENS) and Dipartimento di Chimica "Ugo Schiff", Università di Firenze, I-50019 Sesto Fiorentino, Firenze, Italy; ICCOM-CNR, Istituto di Chimica dei Composti OrganoMetallici, Consiglio Nazionale delle Ricerche, I-50019 Sesto Fiorentino, Firenze, Italy;* orcid.org/0000-0002-6746-696X

Renato Torre − *European Laboratory for Non-Linear Spectroscopy (LENS) and Dipartimento di Fisica e Astronomia, Università di Firenze, I-50019 Sesto Fiorentino, Firenze, Italy;* orcid.org/0000-0003-3182-9906

Complete contact information is available at: https://pubs.acs.org/10.1021/acs.jpclett.0c00363

Notes

The authors declare no competing financial interest.

■ ACKNOWLEDGMENTS

This research was funded by Ente Cassa di Risparmio - Firenze (2016-0866), Ministero dell'Istruzione dell'Università e della Ricerca - Italia (PRIN2017-2017Z55KCW), and European Community by Laserlab-Europe (H2020 EC-GA-654148). We acknowledge M. De Pas, A. Montori, and M. Giuntini for providing their continuous assistance in the setup of the electronics and R. Ballerini and A. Hajeb for the accurate mechanical realizations.

■ REFERENCES

(1) Debenedetti, P. *J. Phys.: Condens. Matter* **2003**, *15*, R1669−R1726.
(2) Gallo, P.; et al. *Chem. Rev.* **2016**, *116*, 7463−7500.
(3) Holten, V.; Anisimov, M. A. *Sci. Rep.* **2012**, *2*, 713−713.
(4) Angell, A. A. *Nat. Mater.* **2014**, *13*, 673.
(5) Soper, A. *Nat. Mater.* **2014**, *13*, 671.
(6) Debenedetti, P. *Nat. Mater.* **2014**, *13*, 663.
(7) Nilsson, A.; Pettersson, L. G. M. *Nat. Commun.* **2015**, *6*, 8998.
(8) Russo, J.; Tanaka, H. *Nat. Commun.* **2014**, *5*, 3556.
(9) Poole, P. H.; Sciortino, F.; Essmann, U.; Stanley, H. E. *Nature* **1992**, *360*, 324−328.
(10) Huang, C.; et al. *Proc. Natl. Acad. Sci. U. S. A.* **2009**, *102*, 15214−15218.
(11) Kim, K. H.; Späh, A.; Pathak, H.; Perakis, F.; Mariedahl, D.; Amann-Winkel, K.; Sellberg, J. A.; Lee, J. H.; Kim, S.; Park, J.; Nam, K. H.; Katayama, T.; Nilsson, A. *Science* **2017**, *358*, 1589−1593.
(12) Sellberg, J. A.; et al. *Nature* **2014**, *510*, 381−4.
(13) Pallares, G.; Azouzi, M. E.; Gonzalez, M. A.; Aragones, J. L.; Abascal, J. L. F.; Valeriani, C.; Caupin, F. *Proc. Natl. Acad. Sci. U. S. A.* **2014**, *111*, 7936−7941.
(14) Taschin, A.; Bartolini, P.; Eramo, R.; Righini, R.; Torre, R. *Nat. Commun.* **2013**, *4*, 2401.
(15) Perakis, F.; Marco, L. D.; Shalit, A.; Tang, F.; Kann, Z. R.; Kuhne, T. D.; Torre, R.; Bonn, M.; Nagata, Y. *Chem. Rev.* **2016**, *116*, 7590−7607.
(16) Prielmeier, F. X.; Lang, E. W.; Speedy, R. J.; Lüdemann, H.-D. *Berichte der Bunsengesellschaft für physikalische Chemie* **1988**, *92*, 1111−1117.
(17) Harris, K. R.; Newitt, P. J. *J. Chem. Eng. Data* **1997**, *42*, 346−348.
(18) Kawamoto, T.; Ochiai, S.; Kagi, H. *J. Chem. Phys.* **2004**, *120*, 5867−70.
(19) Cunsolo, A.; Orecchini, A.; Petrillo, C.; Sacchetti, F. *J. Chem. Phys.* **2006**, *124*, 084503.
(20) Goncharov, A.; Goldman, N.; Fried, L.; Crowhurst, J.; Kuo, I. F.; Mundy, C.; Zaug, J. *Phys. Rev. Lett.* **2005**, *94*, 125508−125508.
(21) Bove, L. E.; Klotz, S.; Strassle, T.; Koza, M.; Teixeira, J.; Saitta, A. M. *Phys. Rev. Lett.* **2013**, *111*, 185901.
(22) Fanetti, S.; Lapini, A.; Pagliai, M.; Citroni, M.; Di Donato, M.; Scandolo, S.; Righini, R.; Bini, R. *J. Phys. Chem. Lett.* **2014**, *5*, 235−240.
(23) Fanetti, S.; Pagliai, M.; Citroni, M.; Lapini, A.; Scandolo, S.; Righini, R.; Bini, R. *J. Phys. Chem. Lett.* **2014**, *5*, 3804−3809.
(24) Lapini, A.; Pagliai, M.; Fanetti, S.; Citroni, M.; Scandolo, S.; Bini, R.; Righini, R. *J. Phys. Chem. Lett.* **2016**, *7*, 3579−3584.
(25) Singh, L. P.; Issenmann, B.; Caupin, F. *Proc. Natl. Acad. Sci. U. S. A.* **2017**, *114*, 4312−4317.
(26) Vedamuthu, M.; Singh, S.; Robinson, G. W. *J. Phys. Chem.* **1994**, *98*, 2222−2230.
(27) Tanaka, H. *J. Chem. Phys.* **2000**, *112*, 799−809.
(28) Tanaka, H. *J. Phys.: Condens. Matter* **2003**, *15*, L703−L711.
(29) Holten, V.; Sengers, J. V.; Anisimov, M. A. *J. Phys. Chem. Ref. Data* **2014**, *43*, 043101.
(30) Holten, V.; Palmer, J. C.; Poole, P. H.; Debenedetti, P. G.; Anisimov, M. a. *J. Chem. Phys.* **2014**, *140*, 104502−104502.
(31) Shi, R.; Russo, J.; Tanaka, H. *Proc. Natl. Acad. Sci. U. S. A.* **2018**, *115*, 9444−9449.
(32) Taschin, A.; Bartolini, P.; Eramo, R.; Righini, R.; Torre, R. *J. Chem. Phys.* **2014**, *141*, 084507.
(33) Torre, R.; Bartolini, P.; Righini, R. *Nature* **2004**, *428*, 296−298.
(34) Ishizumi, A.; Kasami, M.; Mishina, T.; Yamamoto, S.; Nakahara, J. *High Pressure Res.* **2003**, *23*, 201−204.
(35) Krisch, M.; Loubeyre, P.; Ruocco, G.; Sette, F.; Cunsolo, A.; D'Astuto, M.; LeToullec, R.; Lorenzen, M.; Mermet, A.; Monaco, G.; Verbeni, R. *Phys. Rev. Lett.* **2002**, *89*, 125502−125502.
(36) Li, F.; Cui, Q.; He, Z.; Cui, T.; Zhang, J.; Zhou, Q.; Zou, G.; Sasaki, S. *J. Chem. Phys.* **2005**, *123*, 174511.
(37) Bartolini, P.; Taschin, A.; Eramo, R.; Torre, R. Optical Kerr Effect Experiments on Complex Liquids, A Direct Access to Fast Dynamic Processes. *Time-Resolved Spectroscopy in Complex Liquids*; New York, 2008; pp 73−127.
(38) Skaf, M.; Sonoda, M. *Phys. Rev. Lett.* **2005**, *94*, 137802.
(39) DeSantis, A.; Ercoli, A.; Rocca, D. *J. Chem. Phys.* **2004**, *120*, 1657−1658.
(40) Padró, J. A.; Martí, J. *J. Chem. Phys.* **2004**, *120*, 1659−1660.
(41) Ito, H.; Hasegawa, T.; Tanimura, Y. *J. Phys. Chem. Lett.* **2016**, *7*, 4147−4151.
(42) Lang, E. W.; Lüdemann, H. D. *Berichte der Bunsengesellschaft für physikalische Chemie* **1981**, *85*, 603−611.
(43) Arnold, M. R.; Lüdemann, H.-D. *Phys. Chem. Chem. Phys.* **2002**, *4*, 1581−1586.
(44) Wagner, W.; PruSS, A. *J. Phys. Chem. Ref. Data* **2002**, *31*, 387−535.
(45) Mazza, M. G.; Giovambattista, N.; Stanley, H. E.; Starr, F. W. *Phys. Rev. E* **2007**, *76*, 031203.
(46) Kumar, P. *Proc. Natl. Acad. Sci. U. S. A.* **2006**, *103*, 12955−12956.
(47) González, M. A.; Valeriani, C.; Caupin, F.; Abascal, J. L. F. *J. Chem. Phys.* **2016**, *145*, 054505.
(48) Kumar, P.; Franzese, G.; Stanley, H. E. *Phys. Rev. Lett.* **2008**, *100*. DOI: 10.1103/PhysRevLett.100.105701
(49) De Marzio, M.; Camisasca, G.; Rovere, M.; Gallo, P. *Frontiers of Physics* **2018**, *13*, 136103.
(50) Buldyrev, S. V.; Franzese, G. *J. Non-Cryst. Solids* **2015**, *407*, 392−398.
(51) Saitta, A. M.; Datchi, F. *Phys. Rev. E: Stat. Phys., Plasmas, Fluids, Relat. Interdiscip. Top.* **2003**, *67*, 020201.
(52) For the pressure density conversion, we used the data of ref 44. These data cover only the pressure range of the stable liquid phase. Our higher pressure values (620 and 750 MPa at 273 K and 1020 and 1350 MPa at 297 K) fall in the supercooled phase region; we obtain the density values at those pressures by extrapolation from the values in the stable phase.